
# Extension of a Least-Squares Finite Element Method for a Meso-Scale Model of the Spread of COVID-19 for a vaccinated Group

Fleurianne Bertrand[1], Emilie Pirch[2]

[1]*Faculty of Electrical Engineering, Mathematics and Computer Science, University of Twente*
*Zilverling, P.O. Box 217, 7500 AE Enschede, The Netherlands*
*f.bertrand@utwente.nl*
[2]*Dept. of Computational Mathematics, Humboldt-Universität zu Berlin*
*Rudower Chaussee 25, 12439 Berlin, Germany*
*pirchemi@math.hu-berlin.de*

**Abstract.** In this work, we aim at extending our previous findings on a meso-scale SEIRQD model for the spread of COVID-19. The model and its extension are based on the division of the total sum of the living population into different compartments and the virus contraction and recovery dynamics are formulated in a coupled system of PDEs. This system is to be solved by a Least-Squares Finite Element Method and the results will be compared to actual real-life data gathered on the spread of the virus in Germany to evaluate the accuracy of predictions computed with our method. We opt to extend the SEIRQD model by incorporating the growing group of vaccinated individuals. Based on the knowledge on the efficiency of the various vaccines currently in use, we chose to implement this new factor with a certain backflow of vaccinated individuals to the group of exposed individuals to mimic a failure rate, where the vaccination has not been successful.

**Keywords:** COVID-19, least-squares finite element method, SEIRQD

## 1 Model

The point of departure is the meso-scale SEIRQD model for the spread of COVID-19 presented earlier this year in [1]. There, our model assumes that the total living population is divided into five initial compartments: the *susceptible* population $S(\boldsymbol{x}, t)$, the *exposed* population $E(\boldsymbol{x}, t)$, the *infected* population $I(\boldsymbol{x}, t)$, the *recovered* population $R(\boldsymbol{x}, t)$, the *quarantined* population $Q(\boldsymbol{x}, t)$, the *deceased* population $D(\boldsymbol{x})$, and now, newly, the additional group of *vaccinated* individuals $V(\boldsymbol{x})$ is added. Following [2], we denote by $\beta_E, \gamma_E$ the asymptomatic contact and recovery rate and $\beta_I, \gamma_R$ are the infected contact and recovery rate. Moreover, following [3], the deceased group is linearly dependant on the quarantined group and infected enter with a quarantining rate $\delta$. The inverse of the incubation period is $\sigma$, and a backflow of recovered but not immune individuals is implemented with $\eta$. The new parameters associated with the vaccination are the vaccination rate $\mu$, the backflow of "failed" vaccinations is called $\zeta$ and successfully vaccinated individuals are considered "recovered" with a flow rate of $\gamma_V$.
The infection dynamics are implemented in certain in- and out flows of the respective compartment groups. Here, we will only focus on the explanation of the new parameters associated with vaccination and its effects on certain compartments, for details on the other compartments and rates we refer to our previous work [1].

We introduce functions $\phi_i$ sufficiently smooth on a simply connected domain $\Omega \subset \mathbb{R}^2$. For a certain time interval considered, $\phi_i(\boldsymbol{x}, t)$ with $\in \Omega \times [0, T]$ represents the compartments for the formulation of the coupled PDE model for $i \in \{S, E, I, Q, R, D, V\}$. To take a closer look at the dynamics between groups associated with the vaccinated individuals, we follow [4] and assume that the vaccinated and susceptible have a dependency on each other. The vaccination rate $\mu$ directly affects the susceptible group, as vaccinated individuals are, to a certain

extent, considered safe from contracting and also passing on the virus.

$$S \xrightarrow{\mu} V \qquad \frac{\partial}{\partial t}\phi_S \mathrel{-}= \mu S, \quad \frac{\partial}{\partial t}\phi_V \mathrel{+}= \mu S \tag{1}$$

However, considering the limited efficiency of the vaccines, a certain backflow has to be taken into account, as some individuals might still contract the virus.

$$V \xrightarrow{\zeta} E \qquad \frac{\partial}{\partial t}\phi_V \mathrel{-}= \zeta V, \quad \frac{\partial}{\partial t}\phi_E \mathrel{+}= \zeta V \tag{2}$$

The successfully vaccinated individuals are considered "recovered".

$$V \xrightarrow{\gamma_V} R \qquad \frac{\partial}{\partial t}\phi_V \mathrel{-}= \gamma_V V, \quad \frac{\partial}{\partial t}\phi_R \mathrel{+}= \gamma_V V \tag{3}$$

According to our model, the total of the living population is the sum of all the compartments and thus we note

$$n(\boldsymbol{x}) = \sum_{i\in\{S,E,I,Q,R,D,V\}} \phi_i(\boldsymbol{x},t) \tag{4}$$

and implement an Allee effect which expresses that outbreaks of virus contractions tend to occur in large population centers with

$$\frac{\partial}{\partial t}\phi_S(\boldsymbol{x},t) = -f(\phi_S,\phi_E,\phi_I,n(\boldsymbol{x})) \tag{5}$$

and $f(\phi_S,\phi_E,\phi_I,n(\boldsymbol{x})) = \left(1-\frac{\alpha}{n(\boldsymbol{x})}\right)(\beta_I\phi_S(\boldsymbol{x},t)\phi_I(\boldsymbol{x},t)+\beta_E\phi_S(\boldsymbol{x},t)\phi_E(\boldsymbol{x},t))$ with constant parameter $\alpha$, under the assumption that $\phi_i$ are smooth enough to define partial derivatives in space and considering the space of weak derivatives $H^1(\Omega)$.

Now for $[0,T]$ the time interval to be considered and $\boldsymbol{\phi} \in V = L^2(0,T,H^1(\Omega)))^7$, also assuming the population fields are sufficiently smooth, the model consists of the following system of nonlinear coupled partial differential equations over $\Omega \times [0,\, T]$ :

$$\begin{aligned}\frac{\partial}{\partial t}\phi_S(\boldsymbol{x},t) =& \eta\phi_R(\boldsymbol{x},t) + \nabla\cdot(n(\boldsymbol{x})\,\nu_S\nabla\phi_S(\boldsymbol{x},t)) \\ &- \left(1-\frac{\alpha}{n(\boldsymbol{x})}\right)(\beta_I\phi_S(\boldsymbol{x},t)\phi_I(\boldsymbol{x},t)+\beta_E\phi_S(\boldsymbol{x},t)\phi_E(\boldsymbol{x},t)) - \mu\phi_S(\boldsymbol{x},t)\end{aligned} \tag{6}$$

$$\begin{aligned}\frac{\partial}{\partial t}\phi_E(\boldsymbol{x},t) =& \left(1-\frac{\alpha}{n(\boldsymbol{x})}\right)(\beta_I\phi_S(\boldsymbol{x},t)\phi_I(\boldsymbol{x},t)+\beta_E\phi_S(\boldsymbol{x},t)\phi_E(\boldsymbol{x},t)) \\ &- \sigma\phi_E(\boldsymbol{x},t) - \gamma_E\phi_E(\boldsymbol{x},t) + \nabla\cdot(n(\boldsymbol{x})\,\nu_E\nabla\phi_E(\boldsymbol{x},t)) \\ &+ \zeta\phi_V\end{aligned} \tag{7}$$

$$\frac{\partial}{\partial t}\phi_I(\boldsymbol{x},t) = \sigma\phi_E(\boldsymbol{x},t) - \delta\phi_I(\boldsymbol{x},t) - \gamma_R\phi_I(\boldsymbol{x},t) + \nabla\cdot(n(\boldsymbol{x})\,\nu_I\nabla\phi_I(\boldsymbol{x},t)) \tag{8}$$

$$\frac{\partial}{\partial t}\phi_Q(\boldsymbol{x},t) = \delta\phi_I(\boldsymbol{x},t) - \gamma_D\phi_Q(\boldsymbol{x},t) - \gamma_Q\phi_Q(\boldsymbol{x},t) + \nabla\cdot(n(\boldsymbol{x})\,\nu_Q\nabla\phi_Q(\boldsymbol{x},t)) \tag{9}$$

$$\begin{aligned}\frac{\partial}{\partial t}\phi_R(\boldsymbol{x},t) =& \gamma_R\phi_I(\boldsymbol{x},t) + \gamma_E\phi_E(\boldsymbol{x},t) + \gamma_Q\phi_Q(\boldsymbol{x},t) - \eta\phi_R(\boldsymbol{x},t) + \nabla\cdot(n(\boldsymbol{x})\,\nu_R\nabla\phi_R(\boldsymbol{x},t)) \\ &+\gamma_V\phi_V(\boldsymbol{x},t)\end{aligned} \tag{10}$$

$$\frac{\partial}{\partial t}\phi_D(\boldsymbol{x},t) = \gamma_D\phi_Q(\boldsymbol{x},t) \tag{11}$$

$$\frac{\partial}{\partial t}\phi_V(\boldsymbol{x},t) = \mu\phi_S(\boldsymbol{x},t) - \gamma_V\phi_V(\boldsymbol{x},t) - \zeta\phi_V \tag{12}$$

The model is summarized in Figure 1.

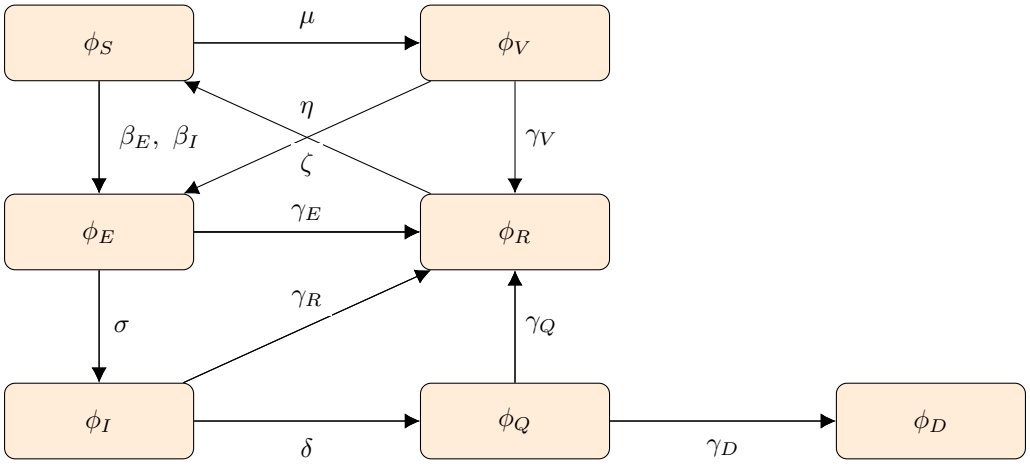


Figure 1. Flow chart depicting the regulating parameter (functions) for the respective compartments of the population $\phi_i$ ($i \in \{S, E, I, Q, R, D, V\}$) and the new vaccination parameters $\mu, \zeta, \gamma_V$.

This system of PDEs can be rewritten in a more convenient vector-matrix notation as $\boldsymbol{\phi} = (\phi_S, \phi_E, \phi_I, \phi_Q, \phi_R, \phi_D, \phi_V)^\top$, $\boldsymbol{\nu} = (\nu_S, \nu_E, \nu_I, \nu_Q, \nu_R, \nu_D, \nu_V)^\top$, $\mathbf{f}(\boldsymbol{\phi}) = (-f(\boldsymbol{\phi}), f(\boldsymbol{\phi}), 0, 0, 0, 0, 0)^\top$, and the parameter matrix

$$\mathcal{P} = \begin{pmatrix} -\mu & 0 & 0 & 0 & \eta & 0 & 0 \\ 0 & -\sigma-\gamma_E & 0 & 0 & 0 & 0 & \zeta \\ 0 & \sigma & -\delta-\gamma_R & 0 & 0 & 0 & 0 \\ 0 & 0 & \delta & -\gamma_Q-\gamma_D & 0 & 0 & 0 \\ 0 & \gamma_E & \gamma_R & \gamma_Q & -\eta & 0 & \gamma_V \\ 0 & 0 & 0 & \gamma_D & 0 & 0 & 0 \\ \mu & 0 & 0 & \gamma_D & 0 & 0 & -\gamma_V-\zeta \end{pmatrix}. \tag{13}$$

Define $\mathcal{D} = n(\boldsymbol{x})diag(\boldsymbol{\nu})$ and set $\boldsymbol{\sigma} = n(\boldsymbol{x})diag(\boldsymbol{\nu})\nabla\boldsymbol{\phi} = \mathcal{D}\nabla\boldsymbol{\phi}$. Then, $\boldsymbol{\sigma}$ is a vector-valued function with components in the space $H_g(\mathrm{div}, \Omega) := \{\boldsymbol{\tau} \in H(\mathrm{div}, \Omega) : \boldsymbol{\tau} \cdot \mathbf{n} = g \text{ on } \partial\Omega\}$ with a Neumann boundary condition $g$ on the boundary $\Gamma = \partial\Omega$ of $\Omega$.Thus, $\sigma$ lies in the discretization space $\Sigma := L^2(0, T, (H_g(\mathrm{div}, \Omega))^7)$.

We define an auxiliary matrix with just two entries in the first line, namely $\beta_E$ and $\beta_I$ and the rest zeroes and multiply it with the factor $(1 - \frac{\alpha}{n})$

$$\mathcal{B} = \left(1 - \frac{\alpha}{n}\right) \begin{pmatrix} 0 & \beta_E & \beta_I & 0 & \dots & 0 \\ & & 0 \in \mathbb{R}^{6\times 6} & & & \end{pmatrix} \tag{14}$$

to then use the definition of $f$ in (5) and get $\mathbf{f}(\boldsymbol{\phi}) = \left(-\boldsymbol{\phi}^\top\mathcal{B}\boldsymbol{\phi}, \boldsymbol{\phi}^\top\mathcal{B}\boldsymbol{\phi}, 0, \dots, 0\right)^\top$.

Then altogether we obtain

$$\frac{\partial}{\partial t}\boldsymbol{\phi} = \mathcal{P}\boldsymbol{\phi} + \mathbf{f}(\boldsymbol{\phi}) + \nabla \cdot \boldsymbol{\sigma}\,. \tag{15}$$

To now discretize in time, an implicit Euler scheme with time step $\tau$ and old time solutions $(\widehat{\boldsymbol{\phi}}, \widehat{\boldsymbol{\sigma}})$ is used to formulate the first-order system as

$$\mathcal{R}(\boldsymbol{\phi}, \boldsymbol{\sigma}; \widehat{\boldsymbol{\phi}}, \widehat{\boldsymbol{\sigma}}) = \begin{pmatrix} \boldsymbol{\phi} - \widehat{\boldsymbol{\phi}} - \tau\left(\mathcal{P}\boldsymbol{\phi} + \mathbf{f}(\boldsymbol{\phi}) + \nabla \cdot \boldsymbol{\sigma}\right) \\ \boldsymbol{\sigma} - \mathcal{D}(\boldsymbol{\phi})\nabla\boldsymbol{\phi} \end{pmatrix} = 0\,. \tag{16}$$

Our Least-Squares Finite Element method aims at a least-squares minimization of $\mathcal{R}(\boldsymbol{\phi}, \boldsymbol{\sigma}; \widehat{\boldsymbol{\phi}}, \widehat{\boldsymbol{\sigma}})$:

search $(\boldsymbol{\phi}, \boldsymbol{\sigma}) \in V \times \Sigma$, such that for all $(\boldsymbol{\psi}, \boldsymbol{\tau}) \in V \times \Sigma$

$$\left\| \mathcal{R}(\boldsymbol{\phi}, \boldsymbol{\sigma}; \widehat{\boldsymbol{\phi}}, \widehat{\boldsymbol{\sigma}}) \right\|_{0,\Omega}^2 \leqslant \left\| \mathcal{R}(\boldsymbol{\psi}, \boldsymbol{\tau}; \widehat{\boldsymbol{\phi}}, \widehat{\boldsymbol{\sigma}}) \right\|_{0,\Omega}^2 . \tag{17}$$

## 2 Finite element discretization and Least-Squares Method

For simplicity and clarity of notation, the finite element discretization of the Least-Squares Finite Element Method is observed for one fixed Euler time step $\tau$. For a triangulation $\mathcal{T}_h$ of $\Omega$, we state the minimization problem (17) in a finite-dimensional subspace $V_h \times \Sigma_h \subseteq H^1(\Omega)^7 \times H_g(\mathrm{div}, \Omega)^7$: search $(\boldsymbol{\phi}_h, \boldsymbol{\sigma}_h) \in V_h \times \Sigma_h$ satisfying

$$\left\| \mathcal{R}(\boldsymbol{\phi}_h, \boldsymbol{\sigma}_h; \widehat{\boldsymbol{\phi}}_h, \widehat{\boldsymbol{\sigma}}_h) \right\|_{0,\Omega}^2 \leqslant \left\| \mathcal{R}(\boldsymbol{\psi}_h, \boldsymbol{\tau}_h; \widehat{\boldsymbol{\phi}}_h, \widehat{\boldsymbol{\sigma}}_h) \right\|_{0,\Omega}^2 \qquad \forall (\boldsymbol{\psi}_h, \boldsymbol{\tau}_h) \in V_h \times \Sigma_h. \tag{18}$$

We choose $V_h = P^1(\mathcal{T}_h)^7$ as the standard Lagrange element and $\Sigma_h = RT^0(\mathcal{T}_h)^7 \cap H_g(\mathrm{div}, \Omega)^7$ the Raviart-Thomas element space accounting for the Neumann boundary condition prescribed by the function $g$. For the case $k = 0$ and $n = 2$, the classical Raviart-Thomas function space of lowest order is given by

$$RT^0(\mathcal{T}_h) := \left\{ q \in P^1(T) : \forall T \in \mathcal{T}_h \ \exists a \in \mathbb{R}^2 \ \exists b \in \mathbb{R} \ \forall x \in T, \ q(x) = a + bx \ \text{ and } \ \forall E \in \mathcal{E}(\Omega), \ [q]_E \cdot n_E = 0 \right\} .$$

At this point, the evident advantage of choosing a Least-Squares Method for this problem is that it does not require some sort of compatibility of the two discretization spaces and thus many problems of theoretical nature can be avoided.

Due to $f$ being a nonlinear function of $\boldsymbol{\phi}$, the discrete problem (18) is a nonlinear least-squares problem that is solved using an inexact Gauss-Newton method of the type of the Gauss-Newton Multilevel Method from [5]. As this method requires a residual-based stopping criterion, we define the residual for the iteration in step $k$ as the simple scalar product

$$\mathrm{res}(\boldsymbol{\phi}_h^{(k)}, \boldsymbol{\sigma}_h^{(k)}) = \left( \mathcal{R}\left( \boldsymbol{\phi}_h^{(k)}, \boldsymbol{\sigma}_h^{(k)}; \widehat{\boldsymbol{\phi}}_h, \widehat{\boldsymbol{\sigma}}_h \right), \mathcal{J}(\boldsymbol{\phi}_h^{(k)}, \boldsymbol{\sigma}_h^{(k)})[\boldsymbol{\psi}_h, \boldsymbol{\tau}_h] \right)_{0,\Omega} . \tag{19}$$

$\mathcal{J}$ is the Fréchet derivative of $\mathcal{R}$ in the direction $[\boldsymbol{\psi}_h, \boldsymbol{\tau}_h] \in V_h \times \Sigma_h$. Note the dependence on the old time solutions $(\widehat{\boldsymbol{\phi}}_h, \widehat{\boldsymbol{\sigma}}_h)$, as the method performs a fixed-point algorithm in each time step. The next aim is to calculate $\mathcal{J}$.

As the nonlinearity is concentrated in the term $\mathbf{f}(\boldsymbol{\phi})$ we define

$$\mathcal{R}_0(\boldsymbol{\phi}, \boldsymbol{\sigma}; \widehat{\boldsymbol{\phi}}, \widehat{\boldsymbol{\sigma}}) = \mathcal{R}(\boldsymbol{\phi}, \boldsymbol{\sigma}; \widehat{\boldsymbol{\phi}}, \widehat{\boldsymbol{\sigma}}) - \tau \left( \mathbf{f}(\boldsymbol{\phi}), 0 \right)^\top \tag{20}$$

in order to simplify the notation and set $\tau = \widehat{\tau}$. For the derivative associated with the variables $\boldsymbol{\sigma}$ and $\boldsymbol{\phi}$ we obtain

$$\frac{\partial}{\partial \theta} \mathcal{R}(\boldsymbol{\phi}, \boldsymbol{\sigma} + \theta \boldsymbol{\tau}; \widehat{\boldsymbol{\phi}}, \widehat{\boldsymbol{\sigma}}) \Big|_{\theta=0} = \begin{pmatrix} \widehat{\tau} \nabla \cdot \boldsymbol{\tau} \\ \boldsymbol{\tau} \end{pmatrix} \quad \text{and} \quad \frac{\partial}{\partial \theta} \mathcal{R}_0(\boldsymbol{\phi} + \theta \boldsymbol{\psi}, \boldsymbol{\tau}; \widehat{\boldsymbol{\phi}}, \widehat{\boldsymbol{\sigma}}) \Big|_{\theta=0} = \begin{pmatrix} \boldsymbol{\psi} - \widehat{\tau} \mathcal{P} \boldsymbol{\psi} \\ -\mathcal{D} \nabla \boldsymbol{\psi} \end{pmatrix} . \tag{21}$$

The analogous directional differentiation in the three components $\phi_{S,E,I}$ of the function $f$ gives the total derivative

$$\frac{\partial}{\partial \theta} f(\boldsymbol{\phi} + \theta \boldsymbol{\psi}) \Big|_{\theta=0} = \left( 1 - \frac{\alpha}{n} \right) \left( \beta_I (\phi_S \psi_I + \psi_S \phi_I) + \beta_E (\phi_S \psi_E + \psi_S \phi_E) \right) . \tag{22}$$

Using matrix $\mathcal{B}$ as defined in (14) and rewriting in matrix notation gives

$$\frac{\partial}{\partial \theta} \mathbf{f}(\boldsymbol{\phi} + \theta \boldsymbol{\psi}) \Big|_{\theta=0} = \left( \boldsymbol{\phi}^T \mathcal{B} \boldsymbol{\psi} + \boldsymbol{\psi}^T \mathcal{B} \boldsymbol{\phi} \right) (-1, 1, 0, \ldots, 0)^\top . \tag{23}$$

Finally, the Fréchet derivative is the sum of the two equations in (21) and (23):

$$\mathcal{J}(\boldsymbol{\phi}, \boldsymbol{\sigma})[\boldsymbol{\psi}, \boldsymbol{\tau}] = \begin{pmatrix} \widehat{\tau} \nabla \cdot \boldsymbol{\tau} + \boldsymbol{\psi} - \widehat{\tau} (\mathcal{P} \boldsymbol{\psi}) - \widehat{\tau} (\boldsymbol{\phi}^T \mathcal{B} \boldsymbol{\psi} + \boldsymbol{\psi}^T \mathcal{B} \boldsymbol{\phi}) \\ \boldsymbol{\tau} - \mathcal{D} \nabla \boldsymbol{\psi} \end{pmatrix} . \tag{24}$$

With the help of this Fréchet derivative (24), the nonlinear least-squares problem (18) can be reformulated to the equivalent variational problem

$$\left(\mathcal{R}\left(\phi_h, \boldsymbol{\sigma}_h\right), \mathcal{J}(\boldsymbol{\phi}_h, \boldsymbol{\sigma}_h)[\boldsymbol{\psi}_h, \boldsymbol{\tau}_h]\right))_{0,\Omega} = 0 \qquad \forall (\boldsymbol{\psi}_h, \boldsymbol{\tau}_h) \in V_h \times \Sigma_h. \tag{25}$$

Successive approximations for steps $k$ and $\boldsymbol{\delta} = (\delta_{\boldsymbol{\phi}_h}, \delta_{\sigma_h})$ are obtained by minimizing the linear least-squares problem

$$\mathcal{F}(\boldsymbol{\delta}; {\boldsymbol{\phi}_h}^{(k)}, {\boldsymbol{\sigma}_h}^{(k)}) = \left\| \mathcal{R}\left({\boldsymbol{\phi}_h}^{(k)}, {\boldsymbol{\sigma}_h}^{(k)}\right) + \mathcal{J}\left({\boldsymbol{\phi}_h}^{(k)}, {\boldsymbol{\sigma}_h}^{(k)}\right) \boldsymbol{\delta} \right\|_{0,\Omega}^2 \tag{26}$$

and minimizing $F$ in $V_h \times \Sigma_h$ is equivalent to the variational formulation

$$\left(\mathcal{R}\left({\boldsymbol{\phi}_h}^{(k)}, {\boldsymbol{\sigma}_h}^{(k)}\right) + \mathcal{J}\left({\boldsymbol{\phi}_h}^{(k)}, {\boldsymbol{\sigma}_h}^{(k)}\right) \boldsymbol{\delta}, \mathcal{J}\left({\boldsymbol{\phi}_h}^{(k)}, {\boldsymbol{\sigma}_h}^{(k)}\right) \boldsymbol{\rho}\right)_{0,\Omega} = 0 \qquad \forall \boldsymbol{\rho} = (\boldsymbol{\psi}_h, \boldsymbol{\tau}_h) \in V_h \times \Sigma_h. \tag{27}$$

The main theorem in [5] states that a stopping criterion based on a particular residual

$$\mathrm{res}(\boldsymbol{\phi}_h^{(k)}, \boldsymbol{\sigma}_h^{(k)}) \leqslant \lambda h \left\| \mathcal{R}\left(\boldsymbol{\phi}_h^{(k)}, \boldsymbol{\sigma}_h^{(k)}\right) \right\|_{0,\Omega} \tag{28}$$

can be used with $\lambda$ a parameter independent of the step-size $h$, if the iterative method at hand converges uniformly with respect to $h$. Thus, our breaking condition for the Gauss-Newton scheme is

$$\mathrm{res}(\boldsymbol{\phi}_h^{(k)}, \boldsymbol{\sigma}_h^{(k)}) = \left(\mathcal{R}\left(\boldsymbol{\phi}_h^{(k)}, \boldsymbol{\sigma}_h^{(k)}; \widehat{\boldsymbol{\phi}}_h, \widehat{\boldsymbol{\sigma}}_h\right), \mathcal{J}\left(\boldsymbol{\phi}_h^{(k)}, \boldsymbol{\sigma}_h^{(k)}\right) [\boldsymbol{\psi}_h, \boldsymbol{\tau}_h]\right)_{0,\Omega} \tag{29}$$

and the method stops as soon as the residual satisfies (28) with $\lambda = 0.2$.

## 3 Parameter Fitting

The parameters mentioned in Section 1 are fitted in a sense that in our first work [1], we have worked with real-life data on political measures taken to slow the spread of the virus. Thus, we assumed that $\alpha, \beta_{E,I}, \delta, \eta$ are linearly dependent on some indicator $\theta(\boldsymbol{x}, t)$ which implements political measures taken in affected areas. In our previous work [1], we designed this indicator with the help of data on flight reduction gathered and made publicly accessible by the Federal Statistical Office of Germany (see [6],[7]). Obviously, the vaccination rate $\mu$ is also dependent on political measures in terms of availability of vaccines and their distribution and the data considering the vaccination rate is found on the website of the *Robert-Koch-Institut* [8].
Parameters that are assumed not to be dependent on political restrictions are constant in time. While linear dependence is a restriction that is important to mention, many established SIR-type models are based on a linear incidence rate such that this ansatz is expected to give first adequate results. Extension to nonlinear functions are expected for follow-up works.

## 4 Numerical Experiment

The aim of the experiment is to check whether the vaccination rates in Germany provided by the *Robert-Koch-Institut* [8] fits the modification of our model. The experiment is two folds: we first used the provided vaccination rates and observe the predicted cases of infection. We start the prediction at March 01, 2021. In Figure 2, a small overestimation can be noted but the model seems to be able to generally take a vaccination rate into account. Secondly, we let the vaccination rate $\mu$ vary in time, fit it with the predictions and compare it to the vaccination rates. Again, a small overestimation can be observed in Figure 3, but roughly our model is able to incorporate the vaccination rate.

## References

[1] F. Bertrand and E. Pirch. Least-Squares Finite Element Method for a Meso-Scale Model of the Spread of COVID-19. *Computation*, vol. , 2021.

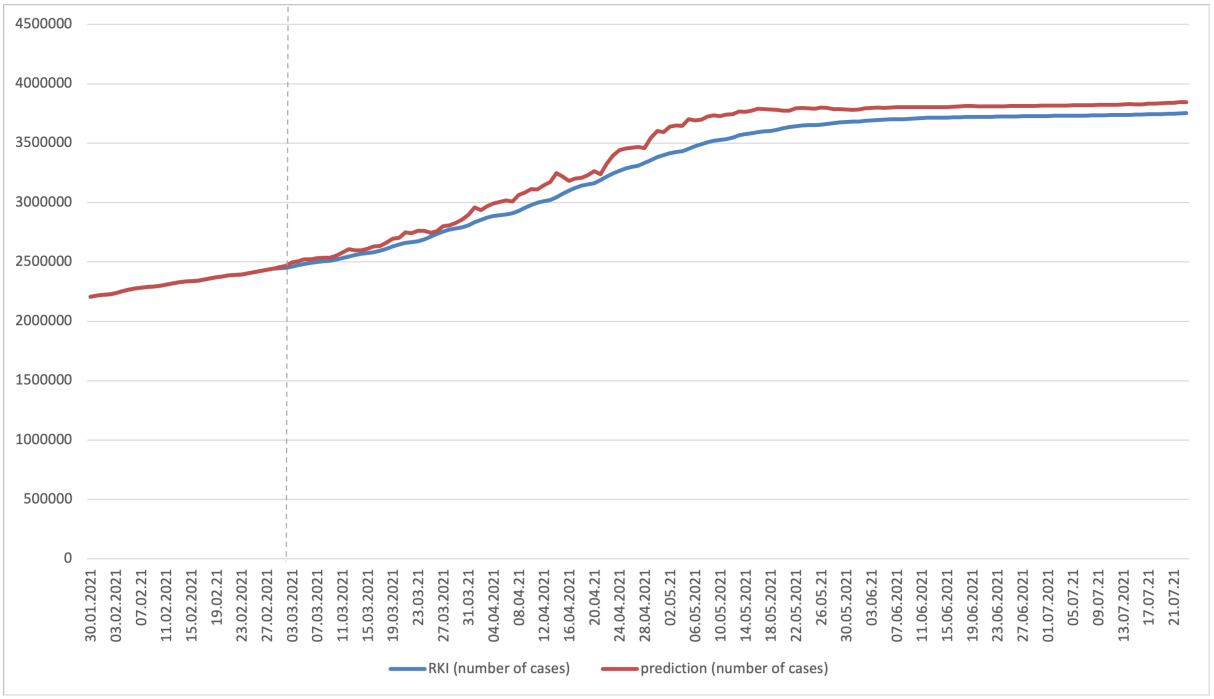


Figure 2. Percentage of infected individuals in the population: data from [8] and predicted

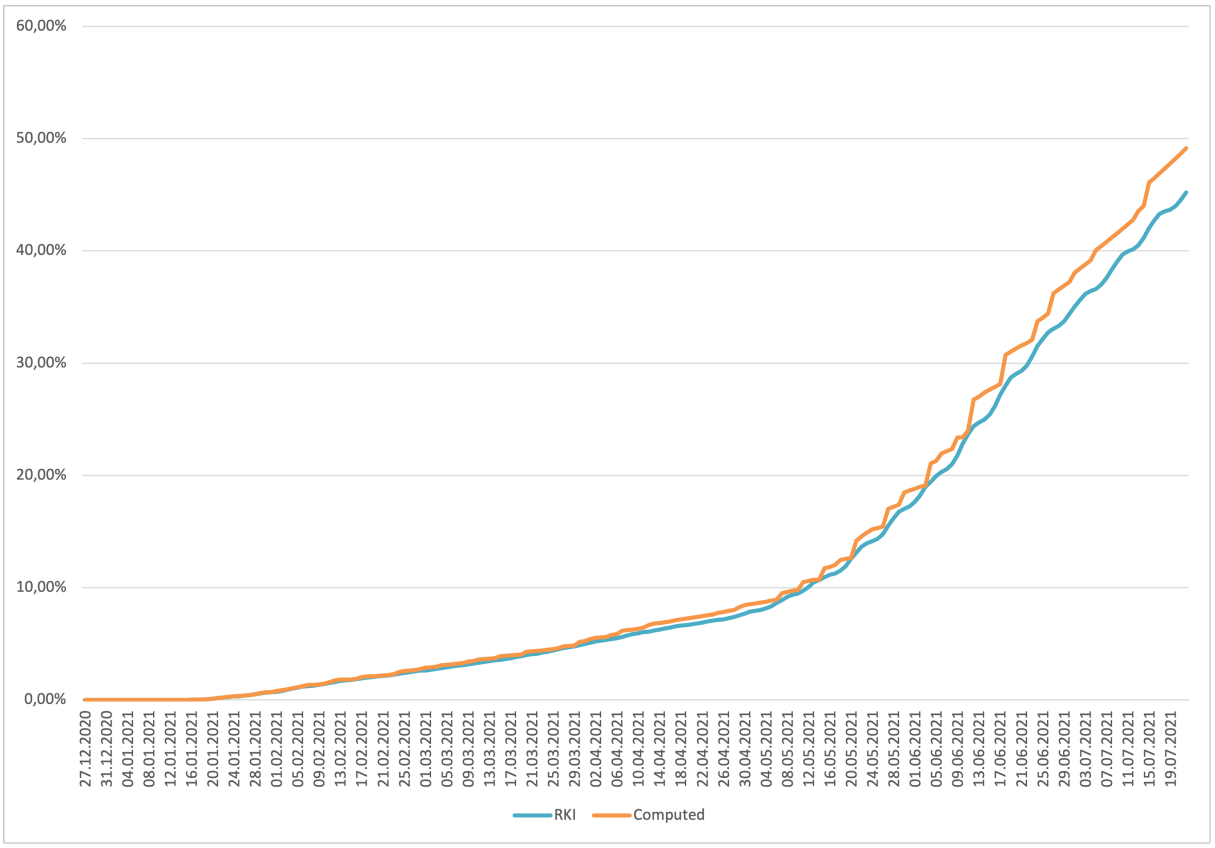


Figure 3. Percentage of vaccinated individuals in the population: data from [8] and computed

[2] A. Viguerie, G. Lorenzo, F. Auricchio, D. Baroli, T. J. Hughes, A. Patton, A. Reali, T. E. Yankeelov, and A. Veneziani. Simulating the spread of COVID-19 via a spatially-resolved susceptible–exposed–infected–recovered–deceased (SEIRD) model with heterogeneous diffusion. *Applied Mathematics Letters 111 106617*, vol. , 2020.
[3] A. Kergaßner, C. Burkhardt, D. Lippold, M. Kergaßner, L. Pflug, D. Budday, P. Steinmann, and S. Budday. Memory-based meso-scale modeling of Covid-19 - County-resolved timelines in Germany. *Computational Mechanics 66:1069–1079*, vol. , 2020.
[4] R. Ghostine, M. Gharamti, S. Hassrouny, and I. Hoteit. An Extended SEIR Model with Vaccination for Forecasting the COVID-19 Pandemic in Saudi Arabia Using an Ensemble Kalman Filter. *Mathematics*, vol. , 2021.
[5] G. Starke. Gauss–Newton Multilevel Methods for Least-Squares Finite Element Computations of Variably Saturated Subsurface Flow. *Computing 64, 323–338*, vol. , 1999.
[6] Statistisches Bundesamt. Luftverkehr auf hauptverkehrsflughäfen. https://www.destatis.de/DE/Themen/Branchen-Unternehmen/Transport-Verkehr/Personenverkehr/Publikationen/Downloads-Luftverkehr/luftverkehr-ausgewaehlte-flugplaetze-2080610197004.pdf?__blob=publicationFile". [Online; accessed October 2020], 2019.
[7] Statistisches Bundesamt. Luftverkehr. https://www.destatis.de/DE/Themen/Branchen-Unternehmen/Transport-Verkehr/Personenverkehr/Publikationen/Downloads-Luftverkehr/luftverkehr-2080600201094.pdf?__blob=publicationFile. [Online; accessed October 2020], 2020.
[8] Robert Koch-Institut Germany. Covid-19 dashboard. https://github.com/robert-koch-institut/COVID-19-Impfungen_in_Deutschland,https://www.rki.de/DE/Content/InfAZ/N/Neuartiges_Coronavirus/Daten/Impfquotenmonitoring.xlsx?__blob=publicationFile. [Online; accessed July 2021], 2021.